

Cite this: *Soft Matter*, 2012, **8**, 7112

www.rsc.org/softmatter

What buoyancy really is. A generalized Archimedes' principle for sedimentation and ultracentrifugation†

Roberto Piazza,^{*a} Stefano Buzzaccaro,^a Eleonora Secchi^a and Alberto Parola^b

Received 15th May 2012, Accepted 26th May 2012

DOI: 10.1039/c2sm26120k

Particle settling is a pervasive process in nature, and centrifugation is a versatile separation technique. Yet, the results of settling and ultracentrifugation experiments often appear to contradict the very law on which they are based: Archimedes' principle – arguably, the oldest physical law. The purpose of this paper is delving into the very roots of the concept of buoyancy by means of a combined experimental–theoretical study on sedimentation profiles in colloidal mixtures. Our analysis shows that the standard Archimedes' principle is only a limiting approximation, valid for mesoscopic particles settling in a molecular fluid, and we provide a general expression for the actual buoyancy force. This “Generalized Archimedes' Principle” accounts for unexpected effects, such as denser particles floating on top of a lighter fluid, which in fact we observe in our experiments.

1 Introduction

Sedimentation of particulate matter is ubiquitous in the natural environment and widespread in industrial processes. For instance, particle and biomass settling is responsible for the formation of depositional landforms¹ and plays a crucial role in marine ecology,² while centrifugation of insoluble solids is a valuable separation method in the extractive, chemical, and food processing industries.³ Thanks to the genius of Jean Perrin, sedimentation studies also provided the key support to the theory of Brownian motion,⁴ and originated powerful methods to investigate soft and biological matter, such as ultracentrifugation, a standard tool to obtain the size distribution of biological macromolecules or to pellet cellular organelles and viruses.⁵ A particle settling in a simple fluid is subjected, besides its weight, to an upward buoyancy force that, according to Archimedes' principle, is given by the weight of the displaced fluid. Usually, however, the settling process involves several dispersed species, either because natural and industrial colloids display a large size distribution or because additives are put in on purpose. The latter is the case of density-gradient ultracentrifugation (DGU), where heavy salts,

compounds like iodixanol, or more recently colloidal nanoparticles, are added to create a density gradient in the solvent. In DGU, proteins, nucleic acids, or cellular organelles are expected to accumulate in a thin band around the position in the cell where the local solvent density matches the density of the fractionated species, the so-called isopycnic point.

DGU is extremely sensitive, allowing for instance to resolve differently labeled genomes with high efficiency,⁶ yet a subtle puzzle recurs in several studies. Even in earlier DGU measurements, the apparent density of some proteins was found to depend on the medium used to establish the density gradient.⁷ The advent of sol-based DGU, allowing not only for more efficient separation of cells^{8,9} but also for fractionation of carbon nanotubes¹⁰ and graphene,¹¹ brought out more striking discrepancies. Indeed, the isopycnic densities of organelles⁸ or carbon nanotubes¹⁰ fractionated using Percoll™, a standard DGU sol, are markedly different from those found in sucrose or salt gradients, and striking anomalies have been observed even for simple polystyrene latex particles.¹² What value should we then take for the density of the medium, to predict the isopycnic point, if the surrounding fluid is not a simple liquid, but rather a complex mixture including other particulate species of different sizes and/or densities? Similar ambiguities exist in experimental and numerical studies of colloidal mixtures settling in fluidized beds,^{13,14} where it is highly debated whether the density ρ of the bare solvent, or rather the density ρ_s of the suspension should be used to evaluate the buoyant force. The latter choice is more widespread, but both attitudes have been taken in the literature,¹⁵ and even empirical interpolating expressions have been suggested to fit experimental data.^{16,17}

The key point of our argument is that, when the suspending fluid is a colloidal suspension or a highly structured solvent, the amount of “displaced fluid” occurring in the simple Archimedes' expression is substantially modified by the density perturbation induced by the particle itself in the surrounding. We shall focus on binary mixtures of particles of types 1 and 2, whose volumes and material densities are, respectively, given by (V_1, ρ_1) and (V_2, ρ_2) , suspended in a solvent of density ρ , under the assumption that component 1 is very diluted. Let us consider, as in Fig. 1, a large spherical cavity of volume \mathcal{V} surrounding a single type-1 particle, and try to extend the common argument used to derive the Archimedes' principle. In the absence of particle 1, mechanical equilibrium requires the total pressure force exerted by the external fluid on \mathcal{V} to exactly balance the weight $W = m_2 n_2 g \mathcal{V}$, where n_2 is the number density of type-2 particles and

^aDepartment of Chemistry (CMIC), Politecnico di Milano, via Ponzio 34/3, 20133 Milano, Italy. E-mail: roberto.piazza@polimi.it

^bDepartment of Science and High Technology, Università dell'Insubria, Via Valleggio 11, 22100 Como, Italy

† Electronic supplementary information (ESI) available. See DOI: 10.1039/c2sm26120k

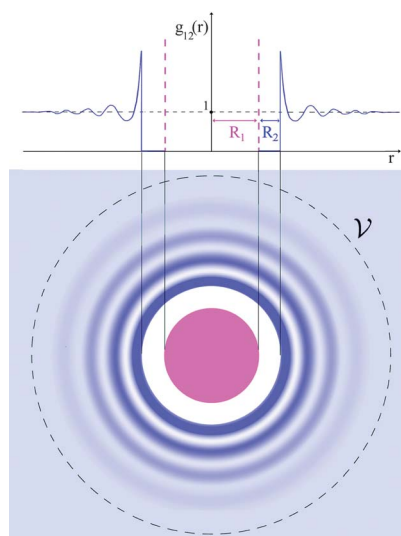


Fig. 1 Schematic view of the density perturbation induced in the surrounding fluid by a settling colloidal particle of radius R_1 , with the upper panel showing the mutual radial correlation function $g_{12}(r)$ of type-2 particles of radius $R_2 = qR_1$. The small q (or low-density) approximation leading to eqn (4) corresponds to evaluated density changes by just taking into account the white “depleted” spherical shell lying between R_1 and R_2 .

$m_2 = (\rho_2 - \rho)V_2$ is their buoyant mass. When particle 1 is inserted, however, the distribution of type-2 particles in \mathcal{V} changes, because interactions generate a concentration profile set by the mutual radial distribution function $g_{12}(r)$, which quantifies the local deviations from uniform density.¹⁸ The total weight of the type-2 particles in \mathcal{V} is now given by $W' = m_2 g_{12} \int_{\mathcal{V}} g_{12}(r) d^3r$. By taking the size of the cavity much larger than the range of $g_{12}(r)$, the total mass contained in \mathcal{V} will then be subjected to an unbalanced mechanical force.‡

$$F_1 = W - W' = -m_2 g_{12} \int [g_{12}(r) - 1] d^3r \quad (1)$$

Provided that the density correlations embodied by $g_{12}(r)$ are fully established, F_1 will also amount to an effective *excess buoyancy force* acting on the test particle, which adds up to the usual Archimedes' term $F_0 = -\rho V_1 g$. This “Generalized Archimedes' Principle” (GAP), which is our main theoretical result, can be equivalently written in terms of purely thermodynamic quantities. Provided that the number density n_1 of type-1 particles is very low, it is indeed easy to show that (see ESI†):

$$F_1 = m_2 g \left(\frac{\partial \Pi}{\partial n_2} \right)^{-1} \left[\frac{\partial \Pi}{\partial n_1} - k_B T \right], \quad (2)$$

where Π is the osmotic pressure of the suspension. Eqn (2) shows that F_1 is proportional to the buoyant mass of type-2 particles and to the osmotic compressibility, whereas the last factor explicitly accounts for mutual interactions between the two components.

For spherical particles of radii R_1 and R_2 , a simple expression for F_1 can be derived provided that component 2 is very diluted too, or, alternatively, that the range of $g_{12}(r)$ is much smaller than R_1 , which is usually the case if the size ratio $q = R_2/R_1 \ll 1$. In this limit, taking $g_{12}(r) = 0$ for $r < R_1 + R_2$, and 1 otherwise, we get $F_1 = (4\pi/3)(R_1 + R_2)^3 n_2 m_2 g$. This result has a simple physical explanation: the excess buoyancy comes from the type-2 particle excluded from the depletion

region shown in white in Fig. 1. The total buoyancy $F_1 + F_0$ yields an “effective” density of the suspending fluid

$$\rho^* = \rho + \Phi_2 (1 + q)^3 (\rho_2 - \rho) \quad (3)$$

where Φ_2 is the volume fraction of type-2 particles. Note that, assuming $\rho_2 > \rho$, ρ^* is always larger than *both* ρ and $\rho_s = \rho + (\rho_2 - \rho)\Phi_2$. Hence, the empirical interpolating expression suggested in ref. 16 is incorrect. A straightforward consequence is that the weight of a type-1 particle is exactly balanced by a suspension of type-2 particles at volume fraction:

$$\Phi_2^* = \frac{\Phi_2^{\text{iso}}}{(1 + q)^3}, \quad (4)$$

which can be substantially *lower* than the isopycnic value $\Phi_2^{\text{iso}} = (\rho_1 - \rho)/(\rho_2 - \rho)$ one would get from assuming that ρ^* is equal to the suspension density. In general, however, the additional force F_1 may not necessarily oppose gravity. A strong attractive contribution to the mutual interaction may indeed overbalance the excluded volume term we considered, reversing the sign of F_1 . Hence, particle 1 can actually be *pulled down* by the surrounding, showing an apparently larger density.

Although derived for colloidal mixtures, eqn (1) is valid under much wider conditions, whenever the region of perturbed solvent density is not negligible compared to V_1 . Moreover, being solely based on a force balance argument, eqn (1) does *not* require the suspension to have reached sedimentation equilibrium, but only that the density distribution of type-2 particles around particle 1 has fully settled. Hence, since the timescale for the latter is usually much faster (at least for Brownian particles), these predictions could be in principle checked on settling mixtures or in fluidized bed experiments. In practice, however, telling apart buoyancy effects from viscous forces is quite hard, because of the presence of long-range hydrodynamic interactions.¹⁹

Thus, to test these ideas, we have devised a targeted *equilibrium* measurement. We have studied model colloidal mixtures, obtained by adding a minute quantity ($\Phi_1 \leq 10^{-5}$) of polymethyl-methacrylate (PMMA, $\rho_1 = 1.19 \text{ g cm}^{-3}$, obtained from microParticles GmbH, Berlin) particles with three different particle sizes ($R_1 \approx 220, 300, 400 \text{ nm}$) to a moderately concentrated suspension of spherical particles with radius $R_2 = 90 \text{ nm}$ made of MFA, a tetrafluoroethylene copolymer with density $\rho_2 = 2.14 \text{ g cm}^{-3}$.²⁰ MFA particles, though spherical and monodisperse, are partially crystalline, and therefore birefringent. Their intrinsic optical anisotropy yields a depolarized component I_{VH} in the scattered light that does *not* depend on inter-particle interactions, but only on the local particle concentration.²⁰ Hence, the full equilibrium sedimentation profile can be simply obtained by vertically scanning a mildly focused laser beam and measuring I_{VH} as a function of the distance from the cell bottom. A simple numerical integration of the experimental profile yields the full equation of state of the system.^{21,22} In addition, MFA has a very low refractive index $n = 1.352$, so it scatters very weakly in aqueous solvents. For better index-matching, we have used as solvent a solution of urea in water at 15% by weight, with density $\rho = 1.04 \text{ g cm}^{-3}$. Hence, at equilibrium, the PMMA particles can be visually spotted as a thin whitish layer lying within a clear MFA sediment.

The equilibrium sedimentation profile of the MFA suspension obtained by depolarized light scattering is shown in the inset of Fig. 2. Using the simple Archimedes' principle, we would expect the PMMA

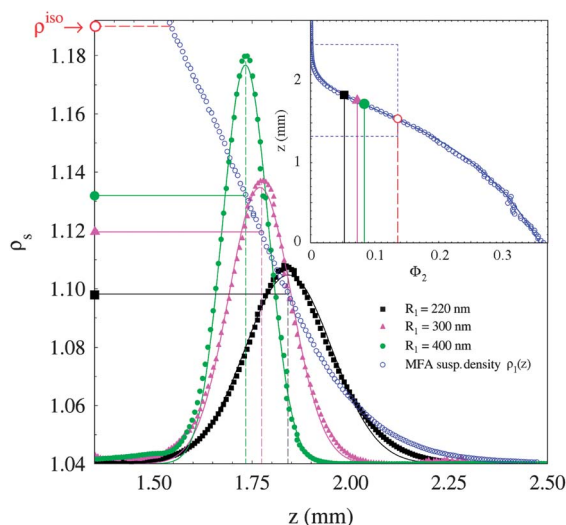


Fig. 2 Inset: equilibrium sedimentation profile of a suspension of MFA particles with radius $R_2 = 90$ nm, dispersed in a solution of urea in water with density $\rho = 1.04$ g cm $^{-3}$. Here z is the distance from the cell bottom, $\Phi_2(z)$ is the local MFA volume fraction, and the full line is the theoretical profile for hard-spheres with a radius $R' \approx 1.1R_2$. In the profile, the mean position of the thin layers of PMMA particles with radius 400 (bullet), 300 (triangle), and 220 nm (square) is compared to the prediction from the simple Archimedes' principle (open dots, corresponding to $\Phi_2 = 0.136$). Main body: expanded view of the profile region within the rectangular box in the inset, showing the local density ρ_s of the MFA suspension. Superimposed are the full distributions (with normalized area) of the PMMA particles obtained from turbidity measurements and fitted with Gaussian distributions as described in the text. Note the location of the isopycnic point where $\rho_s = \rho_2$.

particles to gather around the isopycnic level, namely, the region where the local suspension density is about 1.19 g cm $^{-3}$, which corresponds to $\Phi_2^{iso} = 0.136$. However, the layers lie well above this level, the smaller the PMMA particles are. The distribution of the guest particles can be obtained by evaluating *via* turbidity measurements the sample extinction coefficient through the layer, where the PMMA peak concentration does not exceed $\Phi_1 \approx 10^{-4}$. The body of Fig. 2 shows that the normalized probability distributions for the PMMA particle position have a bell shape centered on anomalously high z -values, with a width that grows with decreasing PMMA particle size. Since the MFA profile changes very smoothly on the scale of the layer thickness, it is in fact easy to show (see ESI†) that the PMMA particles should approximately distribute as a Gaussian with standard deviation:

$$\sigma \approx \sqrt{\Phi_2^* \ell_{g1} \left| \frac{d\Phi_2}{dz} \right|^{-1}}, \quad (5)$$

where $\ell_{g1} = k_B T / m_1 g$ is the gravitational length of the type-1 particles, which we assume to be much larger than R_1 and R_2 . Table 1 shows that the experimental values agree very well with the values predicted by eqn (4), both for the effective isopycnic point Φ_2^* and for the standard deviations of the Gaussian fits.

When considering the opposite case of small, dense particles settling in a “sea” of larger but lighter ones, the GAP yields rather surprising predictions. Eqn (2) shows indeed that F_1 is proportional to the weight of a *large* particle: actually, the density perturbations in

Table 1 Theoretical and experimental values for the effective isopycnic points Φ_2^* and for the standard deviation of the Gaussian fits to the PMMA profiles. Calculated values are based on the simple “excluded volume” approximation leading to eqn (4) and (5), which may be reasonably expected to hold because the values of Φ_2^* are rather small and q is not too large

R_1 (nm)	q	ℓ_{g1} (μ m)	Φ_2^{*theo}	Φ_2^{*exp}	σ^{theo} (μ m)	σ^{exp} (μ m)
220	0.41	63	0.049	0.052	110	113
300	0.30	24	0.062	0.072	78	80
400	0.22	10	0.074	0.083	55	58

the host suspension can generate an excess buoyant force F_1 amounting to a sizable fraction of $m_1 g$, thus yielding an upward push on the small particle that largely *outbalances* its own weight. More specifically, in the ESI† we show that, for hard-sphere mixtures with $q \gg 1$, F_1 is strongly non-monotonic, reaching a maximum at $\Phi_2 < 0.2$. Hence, most of the denser particles will accumulate *atop* the lighter ones § . A striking example of this rather weird effect is shown in Fig. 3, where gold particles, with a radius of about 16 nm and a density $\rho_1 \approx 19.3$ g cm $^{-3}$, are seen to float mostly in the upper, very dilute region of equilibrium sedimentation of MFA particles (here $q \approx 5.6$). The DeLS profile shows that the MFA suspension is actually a colloidal *fluid* (not a solid), with a density as low as $\rho_s \approx 1.2$ g cm $^{-3}$ around the region where most of the gold particles accumulate. Since, for $\Phi_2 \rightarrow 0$, the excess buoyant force F_1 vanishes, some of the latter must lie within the MFA fluid phase too with a concentration profile that decreases downwards, as confirmed by turbidity data. Similarly, gold particles are expected to distribute in the supernatant solvent too, according to a barometric law $c(z) \propto \exp(-z/\ell_{g1})$,

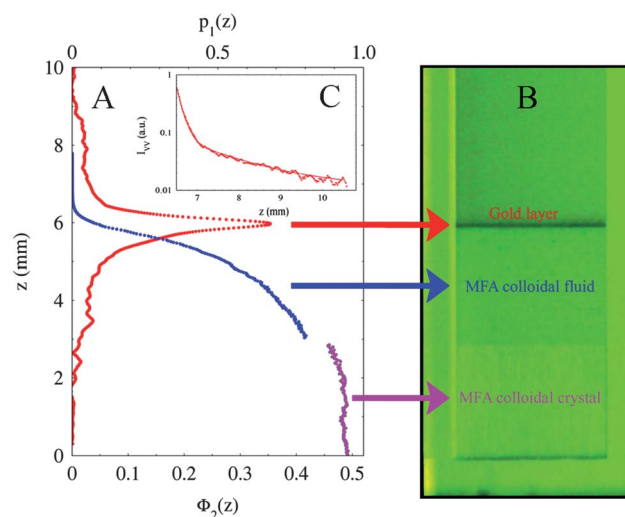


Fig. 3 Equilibrium sedimentation profile (A) and visual appearance (B) of a MFA suspension with a little amount of $R_1 \approx 16$ nm gold particles added. As evidenced by the weak Bragg reflections, the phase closer to the cell bottom is a colloidal crystal, whereas the upper phase is a colloidal fluid. The concentration profile obtained from turbidity data (exploiting in this case the proportionality between gold *absorption* and local concentration) shows that gold particles are also present both within the MFA sediment and in the supernatant solvent. The semilog plot of the polarized scattering intensity in Panel (C) is fitted with a double exponential, as discussed in the text.

with a gravitational length $\ell_{g1} \approx 1.4$ mm. This weak barometric region can be detected by polarized light scattering¶. Panel C in Fig. 3 shows that the polarized scattered intensity can be fitted as the weighted sum of two exponentials $I = I_1 \exp(-z/\ell_{g1}) + I_2 \exp(-z/\ell_{g2})$, where the MFA gravitational length is fixed at the value $\ell_{g2} = 0.13$ mm, whereas from the fit $\ell_{g1} \approx 1.38$ mm for gold. This value for ℓ_{g1} corresponds to an average particle radius $R_1 \approx 16$ nm, which is in very good agreement with the estimate made from the position of the particle plasmonic absorption peak at $\lambda = 528$ nm.

The GAP qualitatively accounts for the anomalous DGU measurements of polystyrene bead density,¹² even when, in the presence of oppositely charged nanoparticles, the latter apparently *increases*, and for empirical expressions used to fit flotation-bed experiments.^{16,17} But eqn (1) has a much wider scope. For instance, provided that a model for g_{12} is available, it should correctly account for “solvation” effects on the buoyancy force felt by proteins, simple molecules, even single ions, or provide a sensitive way to detect DGU aggregation and association effects in biological fluids. Similarly, corrections to the simple Archimedes’ expression will also show up for nanoparticles settling in a strongly correlated solvent, such as a pure fluid or a liquid mixture close to a critical point. Some relation with the Brazil nut effect in granular fluids, which is also affected by the densities of the grain,^{23,24} may also exist, although the latter is usually complicated by the presence of dissipation, convective effects, and effective thermal inhomogeneity. In fact, due to its exquisite sensitivity to the specific properties of a mixture, the “reversed” gravity-segregation effect we have highlighted may allow us to devise novel sophisticated DGU fractionation methods, able to tell apart solutes with the same density and composition, but different size.

We thank D. Frenkel, P. Chaikin, L. Berthier, M. Dijkstra, H. Stone, F. Sciortino, R. Stocker, R. van Roij, A. Philipse, A. van Blaaderen, R. Golestanian, D. Aarts, C. Likos, L. Cipelletti, L. Isa, P. Cicuta, and V. Degiorgio for critical reading of the manuscript, and Solvay Specialty Polymers (Bollate, Italy) for the kind donation of the MFA sample batch. This work was supported by the Italian Ministry of Education and Research (MIUR – PRIN Project 2008CX7WYL).

Notes and references

‡ We assume that the both mutual interactions between the two species and self-interactions between type-2 particles are sufficiently short-

ranged. Eqn (1) is also valid when the host suspension is non-uniform, provided that n_2 varies slowly over the range of $g_{12}(r)$.

§ Note that the accumulation on top of the heavier particles does *not* however lead to a macroscopically inverted density profile. An attentive examination of eqn (1) shows indeed that the weight increase with respect to a suspension of type-2 particles at volume fraction Φ^* , due to the presence of the heavier particles, is exactly balanced by the “expulsion” from the accumulation layer of those particles of type 2 that yield the excess buoyancy F_1 . Macroscopic hydrodynamic stability is thus preserved.

¶ Although in index-matching, MFA particles still scatter polarized light, which is however fully incoherent and proportional to the depolarized scattered intensity.²⁰

- 1 P. Y. Julien, *Erosion and Sedimentation*, Cambridge Univ. Press, Cambridge, 2010.
- 2 T. Kjørboe, *A Mechanistic Approach to Plankton Ecology*, Princeton University Press, Princeton, 2008.
- 3 W. Woon-Fong Leung, *Industrial Centrifugation Technology*, McGraw-Hill Professional, New York, 1998.
- 4 J. Perrin, *Ann. Chim. Phys.*, 1909, **18**, 5.
- 5 J. Lebowitz, M. S. Lewis and P. Schuck, *Protein Sci.*, 2002, **11**, 2067–2079.
- 6 T. Lueders, M. Manefield and M. W. Friedrich, *Environ. Microbiol.*, 2004, **6**, 73–78.
- 7 J. B. Ifft and J. Vinograd, *J. Phys. Chem.*, 1966, **970**, 2814–2821.
- 8 H. Pertoft, *J. Biochem. Biophys. Methods*, 2000, **44**, 1–30.
- 9 O. E. Claassens, R. Menkveld and K. L. Harrison, *Hum. Reprod.*, 1998, **13**, 3139–3143.
- 10 F. Bonaccorso, *et al.*, *J. Phys. Chem. C*, 2010, **114**, 17267–17285.
- 11 A. A. Green and M. C. Hersam, *Nano Lett.*, 2009, **9**, 4031–4036.
- 12 J. Morganthaler and C. A. Price, *Biochem. J.*, 1976, **153**, 487–490.
- 13 L. G. Gibilaro, *Fluidization Dynamics: a Predictive Theory*, Butterworth-Heinemann, Oxford, 2001.
- 14 L. A. M. van Der Wielen, M. H. H. van Dam and K. C. A. M. Luyben, *Chem. Eng. Sci.*, 1996, **51**, 995–1008.
- 15 M. Poletto and D. D. Joseph, *J. Rheol.*, 1995, **39**, 323–343.
- 16 M. C. Ruzicka, *Chem. Eng. Sci.*, 2006, **61**, 2437–2446.
- 17 B. Ž. Grbavčić, Z. L. Arsenijević and R. V. Garić-Grulović, *Powder Technol.*, 2009, **190**, 283–291.
- 18 J.-P. Hansen and I. R. McDonald, *Theory of Simple Liquids*, Elsevier, Amsterdam, 3rd edn, 2006.
- 19 R. Buscall and L. R. White, *J. Chem. Soc., Faraday Trans. 1*, 1987, **83**, 873–891.
- 20 V. Degiorgio, R. Piazza, T. Bellini and M. Visca, *Adv. Colloid Interface Sci.*, 1994, **48**, 61–91.
- 21 R. Piazza, T. Bellini and V. Degiorgio, *Phys. Rev. Lett.*, 1993, **71**, 4267–4270.
- 22 S. Buzzaccaro, R. Rusconi and R. Piazza, *Phys. Rev. Lett.*, 2007, **99**, 098301.
- 23 M. E. Möbius, B. E. Lauderale, S. R. Nagel and H. M. Jaeger, *Nature*, 2001, **414**, 270.
- 24 A. Kudrolli, *Rep. Prog. Phys.*, 2004, **67**, 209–247.

Addition and correction

[View Online](#)

Note from RSC Publishing

This article was originally published with incorrect page numbers. This is the corrected, final version.

The Royal Society of Chemistry apologises for these errors and any consequent inconvenience to authors and readers.
